Lawrence Berkeley National Laboratory
LBL Publications

Title

Electromagnetic Fields in Cased Borehole

Permalink

https://escholarship.org/uc/item/1h4955f2

Authors

Lee, Ki Ha

Kim, Hee Joon

Uchida, Toshihiro

Publication Date

2001-07-01

Copyright Information

ERNEST ORLANDO LAWRENCE
BERKELEY NATIONAL LABORATORY

Electromagnetic Fields in Cased Borehole

Ki Ha Lee, Hee Joon Kim,
and Toshihiro Uchida

Earth Sciences Division

DISCLAIMER

Electromagnetic Fields in Cased Borehole

Ki Ha Lee,[1] Hee Joon Kim,[2] and Toshihiro Uchida[3]
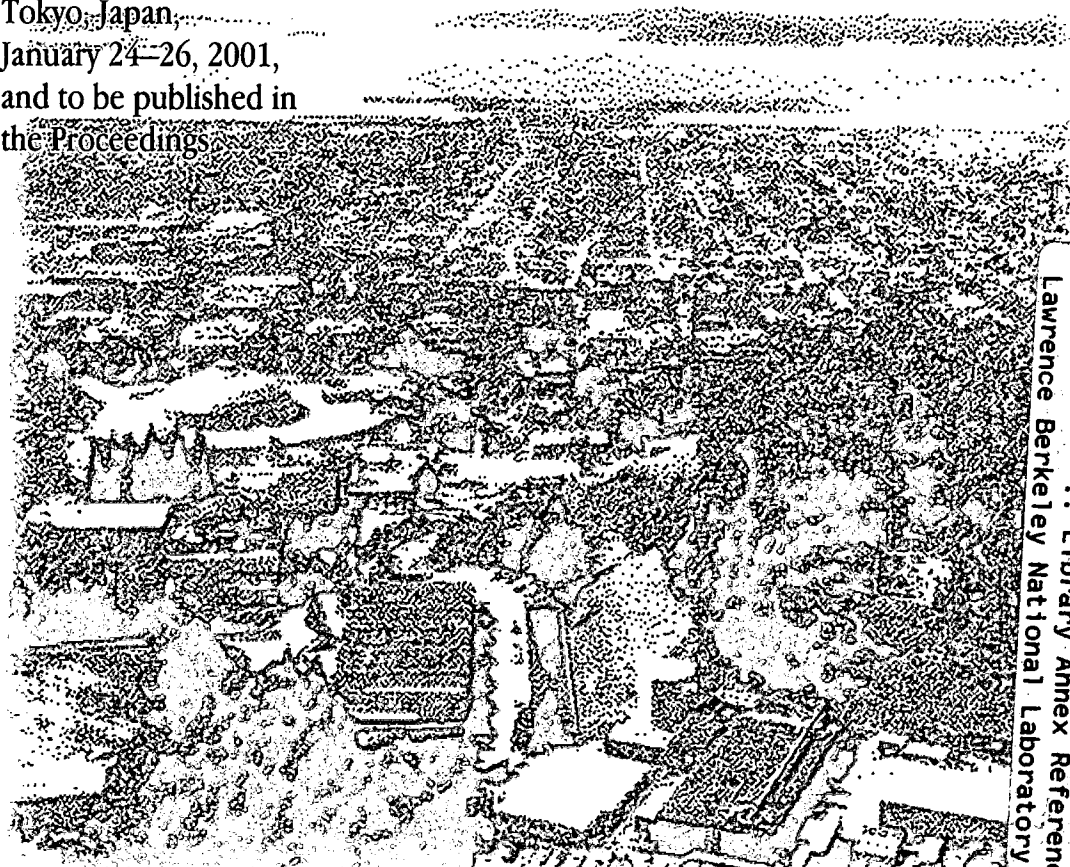
[1]Earth Sciences Division
Ernest Orlando Lawrence Berkeley National Laboratory
University of California
Berkeley, California 94720

[2]Pukyung National University
Pusan, South Korea

[3]Geological Survey of Japan
Tsukuba, Japan

July 2001

Electromagnetic fields in cased borehole

Ki Ha Lee[1)*], Hee Joon Kim[2)], and Toshihiro Uchida[3)]

[1)]*Ernest Orlando Lawrence Berkeley National Laboratory, MS 90-1116, Berkeley, CA 94720 (KHLee@lbl.gov),* [2)]*Pukyung National University, Pusan, S.Korea (hejkim@dolphin.pknu.ac.kr),* [3)]*Geological Survey of Japan, Tsukuba, Japan (uch@gsj.go.jp)*

ABSTRACT

Borehole electromagnetic (EM) measurements, using fiberglass-cased boreholes, have proven useful in oil field reservoir characterization and process monitoring (Wilt et al., 1995). It has been presumed that these measurements would be impossible in steel-cased wells due to the very large EM attenuation and phase shifts. Recent laboratory and field studies have indicated that detection of EM signals through steel casing should be possible at low frequencies, and that these data provide a reasonable conductivity image at a useful scale. Thus, we see an increased application of this technique to mature oil fields, and an immediate extension to geothermal industry as well.

Along with the field experiments numerical model studies have been carried out for analyzing the effect of steel casing to the EM fields. The model used to be an infinitely long uniform casing embedded in a homogeneous whole space. Nevertheless, the results indicated that the formation signal could be accurately recovered if the casing characteristics were independently known (Becker et al., 1998; Lee el al., 1998). Real steel-cased wells are much more complex than the simple laboratory models used in work to date. The purpose of this study is to develop efficient numerical methods for analyzing EM fields in realistic settings, and to evaluate the potential application of EM technologies to cross-borehole and single-hole environment for reservoir characterization and monitoring.

KEY WORDS:borehole, electromagnetic, reservoir characterization, steel casing

INTRODUCTION

Development and testing of the numerical modeling code for an arbitrary casing segment in inhomogeneous conductivity background has been difficult due to the very high electrical conductivity contrast between the steel casing and the background medium. Abnormally high magnetic permeability of the casing further complicates the effort. This requires a very fine numerical grid adjacent to the casing for an accurate solution. At 100 Hz, for example, the grid size needs to be as small as 2 mm to properly discretize a segment of casing commonly used in oil fields. Integral equation method may be considered (Cheryauka and

Sato, 1999), but the numerical complexity caused by the intrinsic coupling of electric and magnetic fields render the approach less attractive. Earlier laboratory and numerical experiments (Augustin et al., 1989; Wu and Habashy, 1994; Wilt et al., 1996; and Becker at al., 1998) indicate that casing effect is local and is only related to the casing nearest the sensor. This conclusion is very useful because, in principle, data obtained through casing can be corrected by considering only the local condition.

To investigate the effect of steel casing efficiently we have developed an accurate but simple finite-element modeling scheme to simulate EM in a medium of cylindrically symmetric conductivity structures. EM fields affected by simple anomalous conductivity distribution in the vicinity of a cased borehole, such as an invaded zone of axial symmetry, can be investigated using this method. One of the main advantages of the approach is that the problem is scalar when formulated using the azimuthal electric field, even if the casing is both electrically conductive and magnetically permeable.

APPROACH

Maxwell's equations with an $e^{+i\omega t}$ time dependence, neglecting displacement currents are written as

$$\nabla \times \vec{E} = -i\omega\mu\vec{H} , \qquad (1)$$
$$\nabla \times \vec{H} = \sigma\vec{E} + \vec{J}_s , \qquad (2)$$

where $\vec{J}_s$ is the impressed current source, and both the magnetic permeability μ and the electrical conductivity σ are heterogeneous. If we let

$$\mu = \mu_b + \delta\mu,$$
$$\sigma = \sigma_b + \delta\sigma ,$$

where the subscript 'b' indicates the background, and let the corresponding electric and magnetic fields

$$\vec{E} = \vec{E}^p + \vec{E}^s ,$$
$$\vec{H} = \vec{H}^p + \vec{H}^s ,$$

1

then, since the primary fields obey

$$\nabla \times \vec{E}^P = -i\omega\mu_0\vec{H}^P,$$

$$\nabla \times \vec{H}^P = \sigma_b\vec{E}^P + \vec{J}_s.$$

the secondary fields $\vec{E}^s$ and $\vec{H}^s$ satisfy

$$\nabla \times \vec{E}^s = -i\omega\mu\vec{H}^s - i\omega\Delta\mu\vec{H}^P, \quad (3)$$

$$\nabla \times \vec{H}^s = \sigma\vec{E}^s + \Delta\sigma\vec{E}^P. \quad (4)$$

The differential equation for the secondary electric field may be derived from equations (3) and (4) as

$$\nabla \times \left(\frac{\nabla \times \vec{E}^s}{\mu} + i\omega\sigma\vec{E}^s\right)$$
$$= -i\omega\Delta\sigma\vec{E}^P + \nabla \times \left(\frac{\Delta\mu}{\mu}\vec{H}^P\right), \quad (5)$$

and the numerical solution for the electric field may be obtained using either the finite-element or the finite difference method. Alternatively, the numerical solution may be obtained using the integral equation method

$$\vec{E} = \vec{E}^P + \oint_V \vec{G}^{EJ} \cdot \vec{J}^s dv + \oint_V \vec{G}^{EM} \cdot \vec{M}^s dv, \quad (6)$$

$$\vec{H} = \vec{H}^P + \oint_V \vec{G}^{HJ} \cdot \vec{J}^s dv + \oint_V \vec{G}^{HM} \cdot \vec{M}^s dv. \quad (7)$$

In the integral equation formulation the electric ($\vec{J}^s = \Delta\sigma\vec{E}$) and magnetic ($\vec{M}^s = \Delta\mu\vec{H}$) scattering currents act like sources in place of the original current source $\vec{J}_s$. Terms $\vec{G}^{EJ}$ and $\vec{G}^{EM}$ are the Green's tensors relating the electric and magnetic scattering currents to the electric field, respectively, whereas $\vec{G}^{HJ}$ and $\vec{G}^{HM}$ relating scattering currents to the magnetic field. A drawback of this approach is that, because of the heterogeneity in both the electrical conductivity and the magnetic permeability, one needs to solve the coupled equations (6) and (7) simultaneously.

Let us consider a small horizontal loop carrying a current $I(\omega)$ as the source in a borehole. If the radius of the loop is a, and it is located at $z = z'$, then the source may be represented in the cylindrical coordinate

$$\vec{J}_s = J_\varphi\vec{\varphi},$$

with

$$J_\varphi = \frac{a}{\rho}I(\omega)\delta(\rho - a)\delta(z - z').$$

Furthermore, let us assume that the electrical and magnetic properties of the earth are cylindrically symmetric about the borehole axis (Figure 1). Then, there exist only one component of electric field, E_φ, and two components of magnetic field, H_ρ and H_z. Here φ, ρ, and z indicate azimuthal, radial, and vertical directions, respectively. Use of the integral equation method would result in having to solve all three components (E_φ, H_ρ, and H_z) simultaneously; a task analogous to obtaining the vector electric field (E_x, E_y, and E_z) in a 3-D heterogeneous conductivity model in Cartesian coordinate. Furthermore, the problem involved is a little more complicated because the coupled equations (6) and (7) require evaluation of both the electric and magnetic field Green's functions.

In this paper we consider the differential equation approach, primarily because the problem under consideration can be reduced to a scalar one. For the geometry considered equation (5) is simplified to

$$\frac{\partial}{\partial z}\left(\frac{1}{\mu}\frac{\partial E_\varphi^s}{\partial z}\right) + \frac{\partial}{\partial \rho}\left[\frac{1}{\mu}\frac{1}{\rho}\frac{\partial(\rho E_\varphi^s)}{\partial \rho}\right] - i\omega\sigma E_\varphi^s,$$
$$= i\omega S_\varphi^p \quad (8)$$

where the source term on the right is shown to be

$$S_\varphi^p = \frac{\Delta\mu}{\mu}(\sigma_b E_\varphi^P + J_\varphi)$$
$$+ \frac{\partial}{\partial z}\left(\frac{\Delta\mu}{\mu}\right)H_\rho^P - \frac{\partial}{\partial \rho}\left(\frac{\Delta\mu}{\mu}\right)H_z^P + \Delta\sigma E_\varphi^P \quad (9)$$

Auxiliary fields, in the total field form, are given by

$$H_\rho = \frac{1}{i\omega\mu}\frac{\partial E_\varphi}{\partial z}, \quad (10)$$

$$H_z = -\frac{1}{i\omega\mu}\frac{1}{\rho}\frac{\partial(\rho E_\varphi)}{\partial \rho}. \quad (11)$$

We use the finite element method (FEM) to solve the differential equation (8) for the electric field E_φ. A variational integral may be derived from the differential equation and, after carrying out the integration in φ, is written as

$$I\left(E_\varphi^s\right) = \oint_S f\left(E_\varphi^s\right)\rho d\rho dz, \quad (12)$$

with

$$f\left(E_\varphi^s\right) = \frac{1}{\mu}\left(\frac{\partial E_\varphi^s}{\partial z}\right)^2 + \frac{1}{\mu}\left[\frac{1}{\rho}\frac{\partial(\rho E_\varphi^s)}{\partial \rho}\right]^2$$
$$+ i\omega\sigma\left(E_\varphi^s\right)^2 + 2i\omega S_\varphi^p E_\varphi^s$$

2

Evaluation of the variational integral in terms of the unknown electric field first involves assigning discrete field variables at nodes of a properly designed grid. A rectangular element is used throughout, and the field is assumed to behave linearly in each of the element. With this assumption, after dropping $( )_v^s$, the electric field in a rectangular element $E^{(e)}$ may be described using a bivariate linear shape function $N = \{N_1, N_2, N_3, N_4\}(\rho, z)$ and the discrete electric fields at four corners $E^{(e)} = \{E_1, E_2, E_3, E_4\}$

$$E^{(e)} = N^T E^{(e)}, \qquad (13)$$

where T indicates transpose of the matrix. Substituting it into the variational integral (12), integrating in ρ and z for each element (Chang and Anderson, 1984), and adding contributions from all elements, one arrives at the numerically equivalent variational integral conveniently written as

$$I(E) = E^T K E - 2 E^T S . \qquad (14)$$

Taking variation of this equation in terms of the discrete electric field, with the boundary condition

$$E|_{\rho=0} = E|_{\rho=\rho_S} = E|_{z=z_T} = E|_{z=z_B} = 0, \qquad (15)$$

one finally obtains the system of linear equations

$$KE = S, \qquad (16)$$

for the secondary electric field at all nodal points of the grid. At the borehole axis the electric field is identically zero. Elsewhere, the boundary condition imposed is the Dirichlet type in which the secondary electric fields at the side ($\rho = \rho_S$), top ($z = z_T$) and bottom ($z = z_B$) boundaries are forced to be zero, a reasonable assumption if the boundary is located far in terms of the skin depth consideration.

NUMERICAL EXAMPLES

Solution to equation (16) is obtained using a Gaussian elimination matrix solver, subject to the boundary condition equation (15). The associated magnetic fields are derived using equations (10) and (11). In order to verify the numerical result, the FEM solution is compared with the analytical solution of EM1D (Lee, 1984, Personal Comm.). The EM1D code is used to calculate electromagnetic fields anywhere in a layered earth for an arbitrary source-receiver polarization. The model chosen for this purpose is a 10 m-thick layer of varying conductivity in an otherwise homogeneous whole space of 0.01 S/m. The magnetic permeability of the layer is fixed at

a value 5 times that of the background, whereas the background value is that of the free-space. The model used for the FEM solution is the whole space in which the layer is included as the anomaly. The source used is a loop of wire of 0.1 m diameter carrying 1 Amp of current at 100 Hertz, and is located 10 m above the top of the layer boundary. In Figures 2, 3 and 4, E_φ, H_ρ, and H_z, respectively, the FEM solution is compared with the EM1D solution along a vertical traverse situated at a horizontal separation of $\rho = 100$ m from the source. In each figure there are two sets of curves, one for the case when the layer conductivity is 1 S/m and the other 10 S/m. For both conductivity contrast models, the real and imaginary parts of all three components of the numerical solution closely match with those calculated from the EM1D. The electric field E_φ and the horizontal magnetic field H_ρ are shown continuous across the layer boundaries, whereas the vertical magnetic field H_z can be seen to be discontinuous because of the contrast in the magnetic permeability.

With the performance of the FEM solution verified, the next step taken is a self-consistency check using a model consisting of a steel casing segment in a whole space of 0.01 S/m. The electrical conductivity of the casing is 10^6 S/m, and the relative magnetic permeability used is 6.25. The inner radius of the casing is 0.1 m and the casing thickness used is 0.01 m. The source used is the same as the one described above. For the consistency check we chose a short 0.2 m long casing segment with the current source located at the center of it. The consistency check involves comparison of two numerical solutions. In one case the whole space is used as the background, and the casing segment is treated as an anomaly. In the other case an infinite casing in the whole space is used as the background, so the upper and lower semi-infinite portions of the casing not occupied by the 0.2 m-long casing segments are now treated as the anomaly. For the purpose of calculating the background field in the presence of the infinite casing, we used the solution by Song and Lee (1998). Figure 5 shows the real and imaginary parts of the vertical magnetic field along a vertical traverse with a horizontal separation of $\rho = 1$ m. The frequency used is 100 Hertz. The agreement between two solutions corresponding to different background settings is obvious, indicating that the FEM solution is self-consistent.

One of the questions regarding the casing effect to the EM fields has been that how long does the casing has to be before it acts as if an infinite casing. To provide a measure of quantitative explanation to this question FEM solutions have been obtained for varying length of the casing segment. Casing properties used are the same as described above. Figure 6 shows the amplitude of the vertical magnetic field normalized by

3

that of the 0.01 S/m whole space. At shorter length the response deviates a little from the whole space response as expected. But as the length is increased to 0.08 m and beyond the response rapidly increases, and reaches its maximum when the length is about 0.3m. As the length gets longer the response appears to be getting smaller, and at about 4 m it seems to be stabilized and becomes close to that of the infinite casing. The behavior has been observed in the laboratory experiment conducted at the Richmond Field Station of UC Berkeley (Becker et al, 1998). Notice that there is a little deviation from the infinite casing as the vertical offset is increased, indicating that some leakage may exist through the ends of the casing segment.

The usefulness of EM methods involving steel-cased borehole for petroleum and geothermal reservoir characterization may be demonstrated using a simple model consisting of a zone of varying conductivity. The conductor is 5 m thick and 20 m wide in radius, axially symmetric about a steel-cased borehole (see the conductor with σ_2 in Figure 1). The whole space is of 0.2 S/m and the frequency used is again 100 Hertz. No anomaly in the magnetic permeability is considered in this case. The source is in the cased borehole and is located at 10 m above the top boundary of the conductor. The resulting numerical solutions for three different conductivity contrasts; 2.5, 5 and 10, are displayed along a traverse separated by 40 m from the transmitter borehole. Figures 7 and 8 show the amplitude and phase of the vertical magnetic field normalized by the whole space response. The amplitude anomaly increases from 1 % to 7 % as the contrast is increased, whereas the peak-to-peak phase anomaly changes from 1° to about 4°. Similar results have been obtained in the transmitter borehole, but the anomaly is essentially negligible with its maximum amplitude of 0.3 % peaking at 18 m below the transmitter. Furthermore, the actual field amplitude decays very quickly and becomes too weak to be measured as the distance is increased rendering the single-hole application difficult. Another numerical test has been made to evaluate the effect of casing irregularity in the vicinity of the transmitter. To simulate variation in casing property a casing collar, 0.1 m long and 0.01 m thick, is attached to the existing casing. The conductive anomaly used outside the casing is the one with its σ_2/σ_1 contrast of 10 (Figure 1). Figures 9 and 10 show the resulting changes in amplitude and phase corresponding to different proximity of the casing collar with respect to the transmitter. Except for the case when the source is right at the casing collar (not shown in this paper), the responses are not much different compared to the one without the collar. It confirms that the casing effect is local, and that the application of cross borehole EM imaging may be practical when only one borehole is steel cased.

CONCLUSIONS

An efficient and accurate FEM numerical solution has been developed to analyze EM fields in the presence of steel casing. All numerical experiments presented in this paper involve axial symmetry in which the source, a horizontal loop, is located inside the cased borehole. Field calculations have been made inside the cased borehole as well as in another borehole which is not cased. Careful analyses of the model results indicate that the anomaly observed in a cross borehole configuration is sensitive enough to be used for the tomographic imaging. It is important to remind that the knowledge of casing property is prerequisite to the proper interpretation of data thus obtained (Becker et al., 1998; Lee et al., 1998). The measurement in a single borehole configuration (not shown in this paper), however, turns out to be insensitive to the formation resistivity. A measurable single-hole anomaly, if existed, may be easily masked off by any combination of irregularities in the casing properties along the length of the borehole.

For common field situations involving cross borehole surveys two boreholes are most likely steel cased. In this case there is no axial symmetry, and the modeling scheme presented in this paper may not be directly applicable for the analysis.

ACKNOWLEDGMENTS

REFERENCES

Augustin, A.M., Kennedy, W.D., Morrison, H.F., and Lee, K.H., 1989, A theoretical study of surface to borehole electromagnetic logging in cased holes: *Geophysics*, **54**, 90-99.

Becker, A., Wang, B., Lee, K.H., and Wilt, M., 1998, Subsurface electromagnetic measurement through steel casing, *Ernest Orlando Lawrence Berkeley National Laboratory*, LBNL-42375.

Cheryauka, A.B., and Sato, M., Nonlinear approximation for EM scattering problem in jointly inhomogeneous medium, *2nd Internat.*

Symp. on Three-Dimensional Electromagnetics (3DEM-2), Oct. 26-29, 1999, Univ. of Utah, Salt Lake City, Utah, 95-98.

Lee, K.H., Kim, H.J., and Song, Y., 1998, Electromagnetic method for analyzing the property of steel casing, *Ernest Orlando Lawrence Berkeley National Laboratory*, LBNL-41525.

Song, Y., and Lee, K.H., 1998, Electromagnetic fields due to a loop current in a cased borehole surrounded by uniform whole space, *Ernest Orlando Lawrence Berkeley National Laboratory*, LBNL-42371.

Uchida, T., Lee, K.H., and Wilt, M.J., 1991, Effect of a steel casing on crosshole EM measurement, *61st Ann. Internat. Mtg., Soc. Expl. Geophys., Expanded Abstracts*, 442-445.

Wilt, M.J., Lee, K.H., Becker, A., Wang, B., and Spies, B., 1996, Crosshole EM in steel-cased boreholes, *66th Ann. Internat. Mtg., Soc. Expl. Geophys., Expanded Abstracts*, 230-233.

Wilt, M.J., Lee, K.H., Morrison, H.F., Becker, A., Tseng, H.-W., Torres-Verdin, C., and Alumbaugh, D., 1995, Crosshole electromagnetic tomography: A new technology for oil field characterization, *The Leading Edge*, 173-177.

Wu, X., and Habashy, T.M., 1994, Influence of the steel casings on electromagnetic signals: *Geophysics*, **59**, 378-390.

Figure 2. Comaprison between FEM and EM1D azimuthal electric field solutions. Blue curves represent the body with 1 S/m, whereas the red curves with 10 S/m.
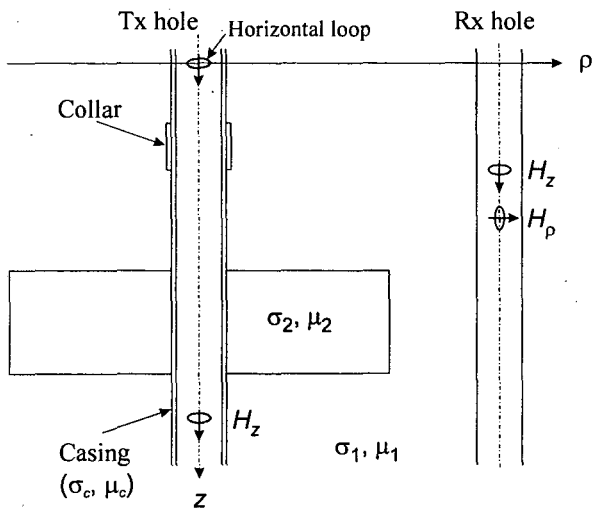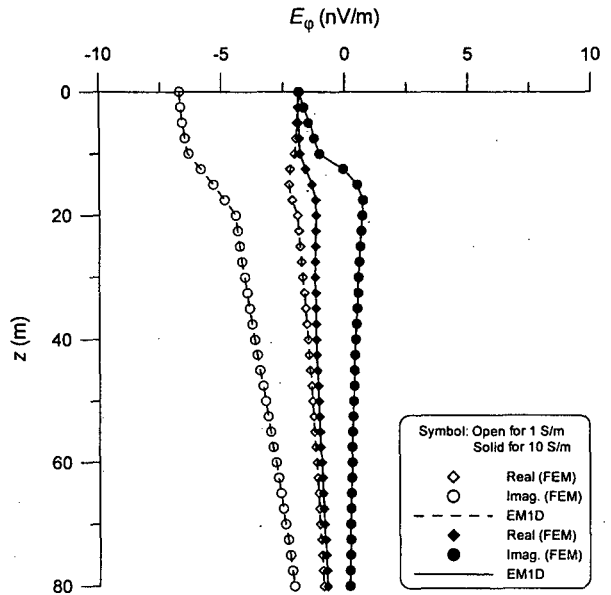

Figure 1. A cylindrically symmetric earth model about a casing segment. Source is a loop of current in the steel cased borehole.
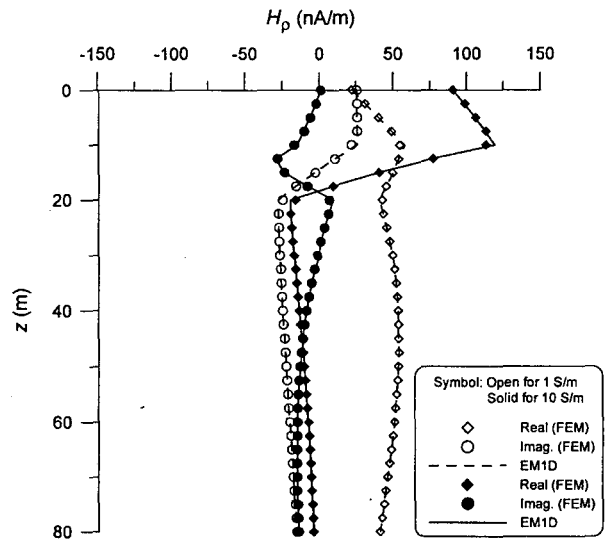

Figure 3. Comaprison between FEM and EM1D radial magnetic field solutions. Blue curves represent the body with 1 S/m, whereas the red curves with 10 S/m.
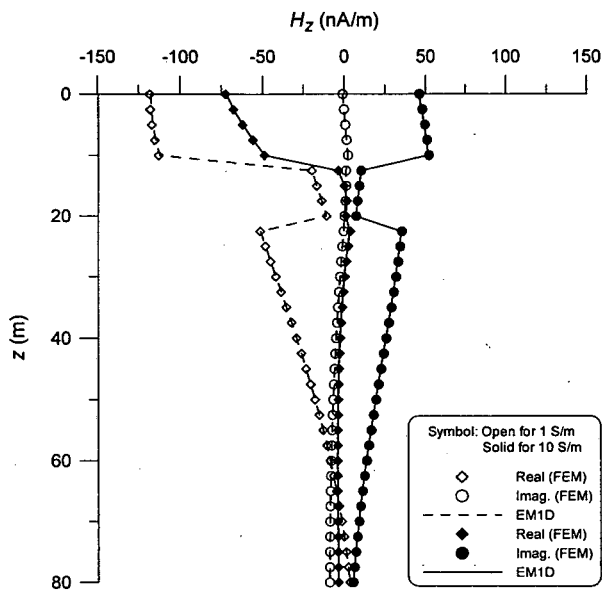
Figure 4. Comaprison between FEM and EM1D vertical magnetic field solutions. Blue curves represent the body with 1 S/m, whereas the red curves with 10 S/m.
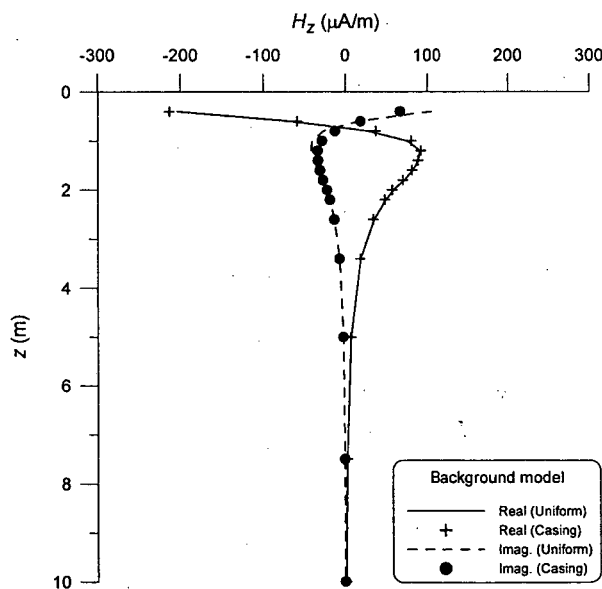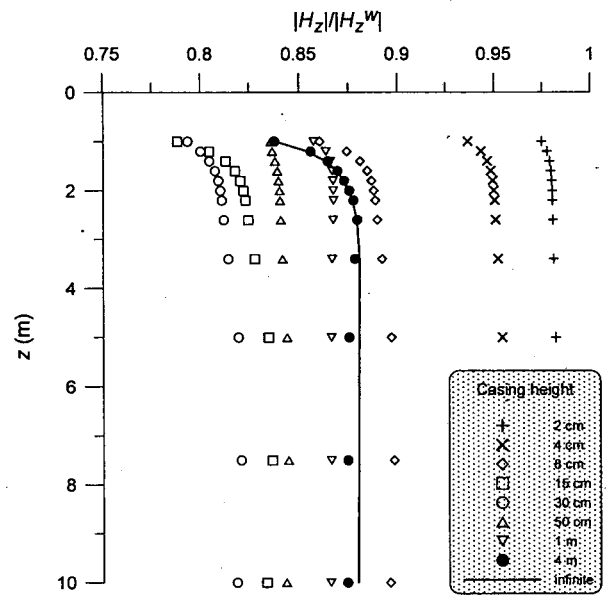

Figure 6. Normalized vertical magnetic field along a vertical traverse for varying casing length. The receiver borehole is horizontally separated by 1 m.

Figure 5. Comparision of numerical solutions for a consistency check using a 0.2 m casing segment. In one case the whole space is used as the background, and the other the infinite casing.
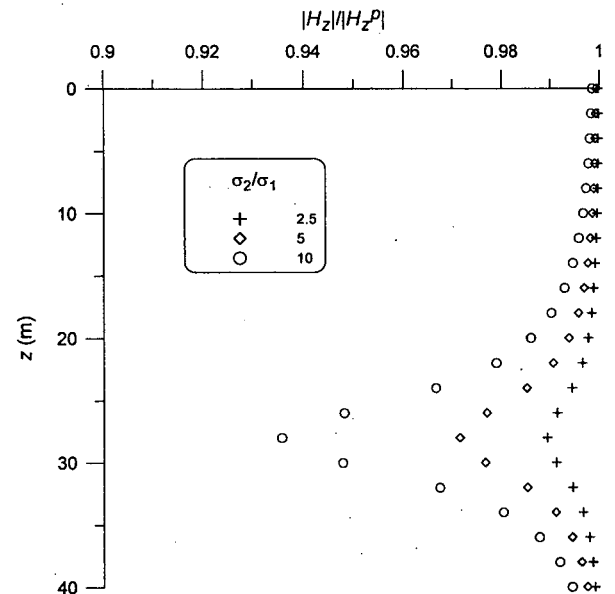

Figure 7. Sensitivity in the amplitude of the vertical magnetic field along a vertical profile 40 m from the transmitter. The anomaly is caused by a conductor 5 m thick and 20 m wide in radius with varying conductivity, in a background of 0.01 S/m.
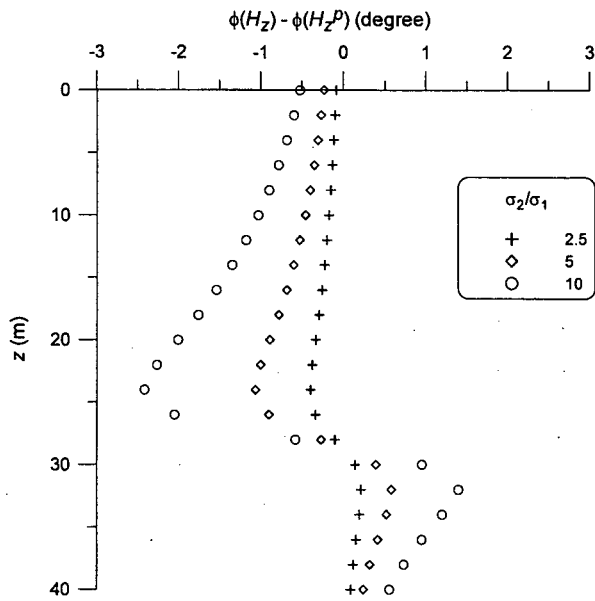
6

Figure 8. Sensitivity in the phase of the vertical magnetic field along a vertical profile 40 m from the transmitter. The anomaly is caused by a conductor 5 m thick and 20 m wide in radius with varying conductivity, in a background of 0.01 S/m.
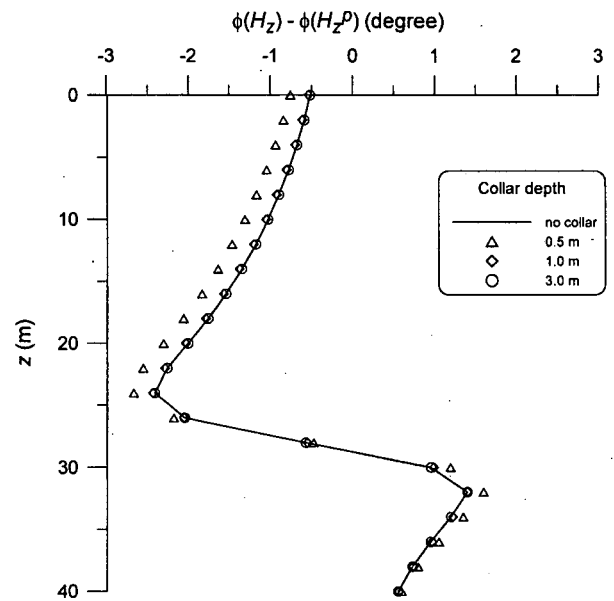

Figure 10. The effect of the casing collar on the phase of the vertical magnetic field associated with the conductor of contrast 10 used in Figures 7 and 8. Different curves indicate different proximity of the color with respect to the source.
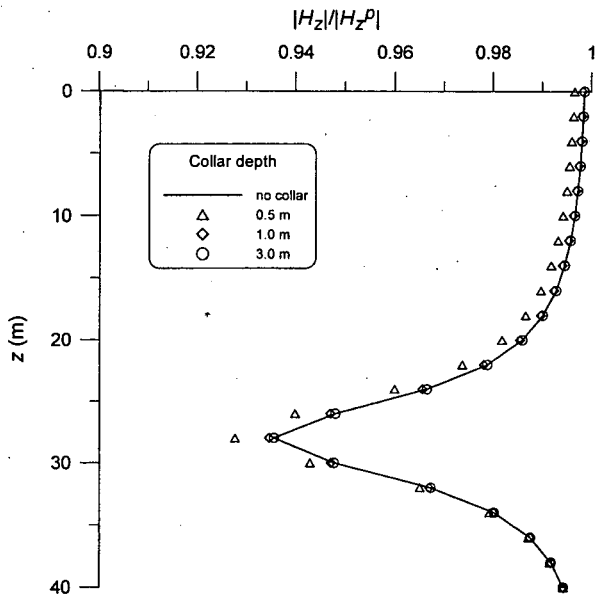

Figure 9. The effect of the casing collar on the amplitude of the vertical magnetic field associated with the conductor of contrast 10 used in Figures 7 and 8. Different curves indicate different proximity of the color with respect to the source.

7